BENDING ELASTIC MODULUS OF RED BLOOD CELL MEMBRANE DERIVED FROM BUCKLING INSTABILITY IN MICROPIPET ASPIRATION TESTS

EVAN A. EVANS
Department of Pathology, University of British Columbia, Vancouver, British Columbia, Canada V6T 1W5

ABSTRACT Observation of cell membrane buckling and cell folding in micropipette aspiration experiments was used to evaluate the bending rigidity of the red blood cell membrane. The suction pressure required to buckle the membrane surface initially was found to be about one-half to two-thirds of the pressure that caused the cell to fold and move up the pipet. A simple analytical model for buckling of a membrane disk supported at inner and outer radii correlates well with the observed buckling pressures vs. pipet radii. The buckling pressure is predicted to increase in inverse proportion to the cube of the pipet radius; also,the buckling pressure depends inversely on the radial distance to the toroidal rim of the cell, normalized by the pipet radius. As such, the pressure required to buckle the membrane with 1×10^{-4} cm diam pipet would be about four times greater than with a 2×10^{-4} cm pipet. This is the behavior observed experimentally. Based on analysis of the observed buckling data, the membrane bending or curvature elastic modulus is calculated to be 1.8×10^{-12} dyn-cm.

INTRODUCTION

It is generally accepted that the mammalian red blood cell can behave as an elastic body. In other words, the red cell can recover its initial biconcave shape after deformation when the external forces that produced the shape change are removed (albeit, the rate of recovery is limited by viscous dissipation in the cell membrane, cytoplasm, and external medium). Because the hemoglobin solution interior to the cell is a liquid, the cell "memory" is associated with the elasticity of the cell membrane. Mechanically, the elastic rigidity of a thin membrane is derived from two sources (Evans and Skalak, 1980): (*a*) free energy change due to deformation (stretch) of the membrane as a flat surface; (*b*) free energy change due to curvature change (bending) of the membrane. Because of the strong hydrophobic interactions of the membrane amphiphiles and the adjacent aqueous media, the cell membrane greatly resists area dilation; hence, the primary surface deformation is shear (i.e., stretch or extension of the surface at constant surface area where a square element of surface becomes a rectangle of the same area). Consequently, deformation of the flaccid red cell is resisted by the bending and shear rigidities of the membrane. Each rigidity is associated with an elastic modulus; e.g., μ is the elastic shear modulus (dyn/cm) for in-plane extension and B is the curvature or bending elastic modulus (dyn-cm) of the membrane. An elastic membrane may be dominated by either the bending or shear rigidities; for example, a phospholipid bilayer with fluid acyl chains has no surface shear rigidity, only bending resistance. However, for the red cell membrane, the ratio of bending to shear rigidity depends on the choice of experiments used to evaluate red cell deformability. Experiments that involve significant curvature changes with little surface extension indicate a large bending rigidity, but experiments that produce significant surface extension appear to be dominated by extensional, or shear, rigidity of the membrane. Deformations that produce only small surface extensions include osmotic swelling of red cell disks (Evans, 1973 *a*; Deuling and Helfrich, 1976; Jenkins, 1977; Zarda et al., 1977; Fischer et al., 1981) and the low-shear onset for "tank-treading" of a biconcave red cell disk in a fluid shear field (Schmid-Schönbein and Gaehtgens, 1981; Fischer et al., 1981). Some of the authors cited have interpreted the cell response as demonstration of large membrane bending rigidity (Fischer et al., 1981; Schmid-Schönbein and Gaehtgens, 1981; Deuling and Helfrich, 1976). Other experiments, like micropipette aspiration and end-to-end extension of red cells, produce large surface extension. Here, the resistance to deformation has been correlated with the surface shear rigidity (Evans, 1973 *b*; Hochmuth et al., 1973; Chien et al., 1978; Waugh and Evans, 1979). The analytical attempts to evaluate the bending to shear rigidity ratio for red cell membrane have also been divided along the lines of the two previously mentioned experiments (Zarda et al., 1977; Evans, 1980; Fischer et al., 1981). Clearly, what has been missing is an experiment where bending and shear effects are directly observable. Such an experiment, where these membrane

rigidities are of comparable magnitude and the significance of both properties are demonstrated, will be briefly described and analyzed below.

When a flaccid red cell is aspirated into a small micropipette, the cell projection inside the pipet increases uniformly with increasing suction pressure. At a specific aspiration length, the cell membrane buckles (folds) and the cell rapidly enters the pipet until limited by surface area and volume restrictions. Fig. 1 shows video micrographs of a single cell aspiration before and after buckling: *a*, *b*, and *c* are side views; *d*, *e*, and *f* are top views. *b* and *e* show the appropriate views just before the cell folds and enters the pipet, and the final state is shown in *c* and *f*. All of the views are of cells at mechanical equilibrium; that is, the shapes are not changing with time. (The cell in *a*, *b*, and *c* is not the same cell as in *d*, *e*, and *f*, because the latter required the use of a curved micropipette.) Buckling is an instability where the membrane bending rigidity is not sufficient to prevent deflections normal to the surface, when the membrane is subject to in-plane compression. A simple example is to take a thin, cardboard sheet and compress it end-to-end: observe the instability. Simple geometric analysis of the pipet aspiration experiment (Evans and Skalak, 1980) shows that the membrane is extended along the radial direction normal to the pipet axis and is compressed along directions tangent to circles centered on this axis. Hence, the total surface area remains constant. If the shear rigidity of the membrane were negligible, then no buckling would occur; the aspirated shapes would remain axisymmetric. On the other hand, if the bending rigidity were negligible, the membrane would wrinkle and fold immediately upon entrance into the micropipette (witness a vacuum cleaner hose applied to a thin rubber sheet). Clearly,both properties are in evidence here.

EXPERIMENTAL AND ANALYSIS

The experiment, illustrated in Fig. 1, was to determine the aspiration pressure and length where red cell membrane buckling occurred. Because buckling was observed to depend strongly on the pipet diameter, pipet inner diameters in the range of 1×10^{-4} to 2×10^{-4} cm were used. The inner diameter of a pipet was measured from the insertion depth of a microneedle that was calibrated by scanning electron microscope. Fig. 2 shows the aspiration pressures where (*a*) membrane buckling was first observed, and (*b*) the cells became unstable, folded, and moved further into the pipet. These data are plotted against the pipet radius. Each observation was reproducible, with little variance for a given pipet and cell size. The scatter shown in Fig. 2 reflects the variation in cell diameter and deviation from axial symmetry (i.e., the pipet not exactly centered). It is important to note that buckling was initiated consistently at pressures about one-half to two-thirds of the level required to fold the cell (also shown in Fig. 2). This was deduced from the top-view experiments; note the difference between Figs. 1, *d* and *e*. Figs. 1 *a* and 1 *b* correspond to Figs. 1 *d* and 1 *e* in aspiration pressure and length. It appeared that the curved, outer rim of the cell opposed the buckling of the interior membrane region. However, even in the slightly buckled (prefold) state, the cell geometry was time independent. Thus, the pressure level required to fold the cell is a conservative upper bound for this type of buckling instability. Because of the complexity associated with top-view observations (e.g., the use of curved pipets and differential interference contrast microscopy to enhance the surface topography), it is preferable to use the side-view observation of cell instability and folding to quantitate the buckling process. (Further details on the pipet aspiration experiment can be found in Waugh and Evans, 1979, or Evans and Skalak, 1980.)

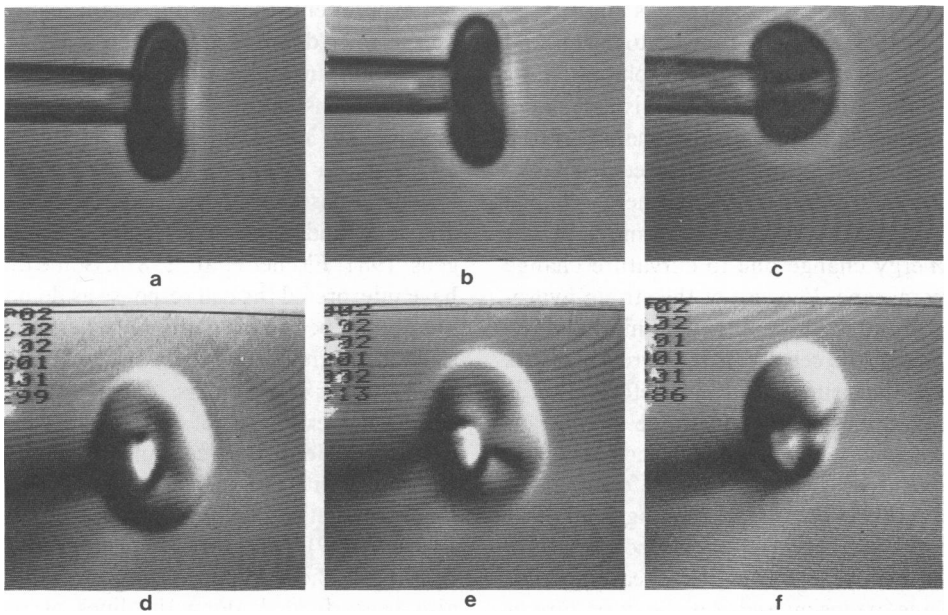

FIGURE 1 Video micrographs of a single red blood cell aspiration by micropipet. *a* and *b* are side views before and *c* is after the cell folded and moved up the pipet ($\sim 1.0 \times 10^{-4}$ cm). *d*, *e*, and *f* are corresponding top views (with a 1.2×10^{-4} cm pipet,but not the same cell). *a* and *d* are equilibrium shapes at pressures (900 and 650 dyn/cm^2, respectively) where membrane buckling appeared to occur initially. *b* and *e* are metastable shapes at pressures (1,400 and 990 dyn/cm^2, respectively) just before the cells folded. (The micrographs were made using a 40x long working-distance objective, NA 0.65, and interference contrast optics.)

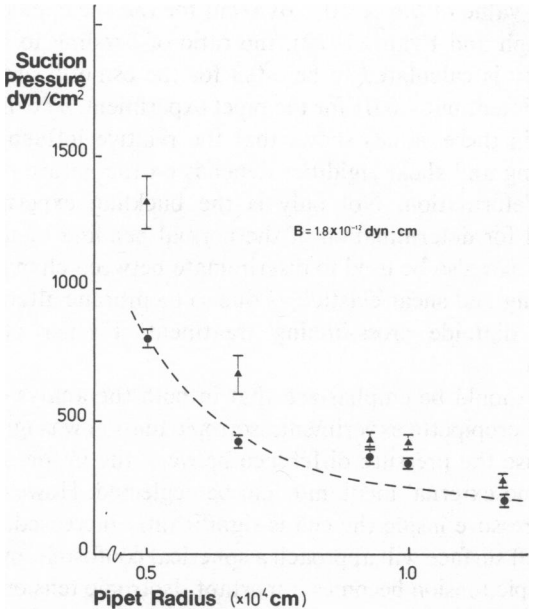

FIGURE 2 Data for aspiration pressure where the cells became unstable, folded and moved up the pipet (▲), and where the cell membrane appeared to buckle initially (•), plotted against pipet inner radius. ---, the correlation with the theoretical prediction for the onset of buckling.

It is not presently possible to analyze the complicated geometry that follows membrane buckling. However, it is possible to investigate the onset of buckling with a perturbation analysis. The approach described below considers the aspiration of a flat, circular disk of membrane that is supported at an inner diameter given by the pipet entrance and at the outer diameter given by the toroidal rim of the cell. This "drum-head" idealization is illustrated in Fig. 3. The support condition at the outer rim is based on the experimental observation that the curvature at the rim acts to "stiffen" the membrane, hence to support the inner disk region of the cell membrane. First, the unperturbed equations of mechanical equilibrium for the membrane must be established for the balance of forces tangent to the membrane plane(Evans and Skalak, 1980):

$$\frac{\partial}{\partial r}(r \cdot T_m^\circ) - T_\phi^\circ = 0. \tag{1}$$

The normal force balance is identically zero since there is no curvature and negligible pressure difference. In the unperturbed (axisymmetric) case, the principal force resultants (membrane tensions) are given by T_m° and T_ϕ°, where T_m° in the tension that acts along the radial direction in the circular disk and T_ϕ° is the circumferential tension that acts tangent to circles defined by the radius, r. The solution to Eq. 1 is

$$T_m^\circ = C_o + C_1/r^2,$$
$$T_\phi^\circ = C_o - C_1/r^2.$$

The first term, C_o, is a surface isotropic (liquidlike) tension at the periphery, which is related to pressure build-up inside the cell. The second, C_1/r^2, is the surface shear resultant. Numerical analysis of the micropipette aspiration test (Evans, 1980) has shown that the first term, C_o, can be neglected, provided the cell is not forced to become spherical. The second term is given by the tension at the pipet entrance:

$$T_m^\circ \simeq \Delta P \cdot R_p^3/(2r^2),$$
$$T_\phi^\circ \simeq -\Delta P \cdot R_p^3/(2r^2), \tag{2}$$

where ΔP is the pipet suction pressure. With the elastic constitutive relation for membrane shear, the meridional tension at the pipet entrance

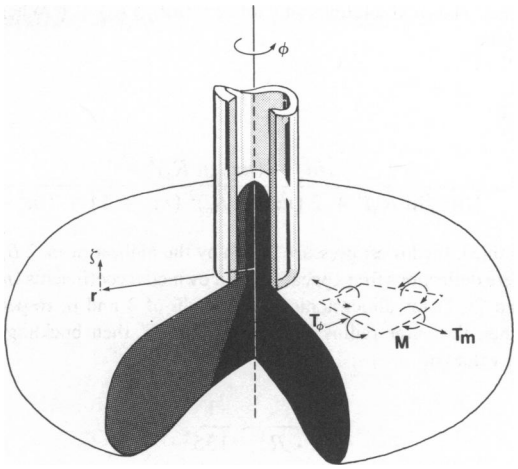

FIGURE 3 Schematic illustration of the membrane aspiration model. In the model, a flat circular region of the membrane is assumed to be supported at the pipet rim and the outer periphery defined by the toroidal rim of the cell ($r = R_o$). The actions of membrane force and moment resultants are sketched on the surface.

can be approximately related to the shear modulus by $T_m^\circ \sim \mu \cdot L/R_p$, where μ is the elastic shear modulus (dyn/cm) of the membrane and L is the aspiration length inside the pipet.

The next step is to examine possible solutions to the equations of mechanical equilibrium perturbed by a deflection, ζ, normal to the disk. In the linearized limit of small perturbations, only the balance of normal forces needs to be considered:

$$-\nabla^2 M + T_m^\circ \cdot k_m + T_\phi^\circ \cdot k_\phi = 0 \tag{3}$$

where M is the bending moment that is introduced by curvature (Evans and Skalak, 1980); k_m and k_ϕ are the principal membrane curvatures given by the approximation

$$k_m \simeq -\frac{\partial^2 \zeta}{\partial r^2},$$
$$k_\phi \simeq -\frac{1}{r}\frac{\partial \zeta}{\partial r} - \frac{1}{r^2}\frac{\partial^2 \zeta}{\partial \phi^2}.$$

Likewise, the bending moment is approximated by the Laplacian, ∇^2, of the deflection (proportional to the total curvature $k_m + k_\phi$),

$$M \simeq -B \cdot \nabla^2 \zeta, \tag{4}$$

where B is the bending or curvature elastic modulus (dyn-cm) of the membrane. With the use of Eqs. 2–4, the perturbed normal force balance is given by

$$B \cdot \nabla^4 \zeta - \left(\frac{\Delta P \cdot R_p^3}{2}\right)\left(\frac{1}{r^2}\frac{\partial^2 \zeta}{\partial r^2} - \frac{1}{r^3}\frac{\partial \zeta}{\partial r} - \frac{1}{r^4}\frac{\partial^2 \zeta}{\partial \phi^2}\right) = 0. \tag{5}$$

For the disk supported at both inner ($2R_p$) and outer ($2R_o$) diameters, Eq. 5 admits solutions of the form, $\zeta \sim \tilde{r} \cdot \sin(n\pi \cdot \ln \tilde{r}/\ln \tilde{R}_o) \cdot \sin m\phi$, where dimensionless expressions for the radii, $\tilde{r} = r/R_p$ and $\tilde{R}_o = R_o/R_p$, have been introduced. (This solution is appropriate to the boundary conditions $\zeta = 0$ at $r = R_p$ and R_o.) With this solution, Eq. 5 reduces to an algebraic relation:

$$\frac{2B}{\Delta P \cdot R_p^3}[(n\pi/\ln \tilde{R}_o)^4 + 2(n\pi/\ln \tilde{R}_o)^2(m^2+1) + (m^2-1)^2]$$
$$= m^2 - (n\pi/\ln \tilde{R}_o)^2 - 1. \tag{6}$$

Clearly, Eq. 6 has real solutions only for $m > (n\pi/\ln \tilde{R}_o) + 1$. When Eq. 6 is rewritten,

$$\frac{2B}{\Delta P \cdot R_p^3} = \frac{m^2 - (n\pi/\ln \tilde{R}_o)^2 - 1}{[(n\pi/\ln \tilde{R}_o)^4 + 2(n\pi/\ln \tilde{R}_o)^2 (m^2 + 1) + (m^2 - 1)^2]}$$

and examined, the lowest pressure [given by the highest ratio, $2B/(\Delta P \cdot R_p^3)$] where deflections first appear is given by modal coefficients (m, n) of (5, 1) and (3, 1) for dimensionless outer radii of 3 and 6, respectively. Thus, when the outer radius is three pipet radii, then buckling would occur for values of

$$\frac{B}{\Delta P \cdot R_p^3} \sim \frac{1}{135}, \tag{7}$$

and when the outer radius is six pipet radii, the buckling would occur for

$$\frac{B}{\Delta P \cdot R_p^3} \sim \frac{1}{55}. \tag{8}$$

The most important prediction of the analysis is that the pressure where buckling is initiated depends strongly on the pipet radius. The dashed line in Fig. 2 is the correlation of the prediction from Eq. 6 with the experimental results for a specific value of $B = 1.8$ dyn-cm. As noted previously, the data correspond to pressures that appear to buckle the membrane initially. A representative value of 3×10^{-4} cm was used for the radial distance to the toroidal rim, R_o. Thus, on the basis of the buckling experiment and analysis, the red cell membrane bending modulus is estimated to be $\sim 1.8 \times 10^{-12}$ dyn-cm.

CONCLUSIONS

Cell membrane buckling and cell folding in pipet aspiration experiments can be used to test the ratio of bending to shear rigidity of red cell membrane. The observation of the pressure where the cell folds can be used to quantitate the rigidity ratio if it is recognized that the pressure required to buckle the membrane initially is 30–50% lower. The simple analysis for aspiration of a membrane disk supported at inner and outer radii predicts the dependence of the buckling pressure on the pipet radius and cell size well. Correlation of the analysis with the experimental data yields a value of 1.8×10^{-12} dyn-cm for the membrane bending modulus. This value is consistent with the bound inferred previously from the intercept of the pipet suction pressure vs. aspiration length data (Evans, 1980). In general, the local ratio of bending to shear ridigity can be represented by the dimensionless parameter, $B/(\mu \cdot \epsilon_s \cdot R^2)$, where ϵ_s is the local level of surface extension or shear deformation, and R is the local radius of curvature. In pipet experiments, surface extension ratios close to the pipet entrance can be as large as 2 or 3 to 1, which is equivalent to values of 2 to 4 for the shear strain. On the other hand, in osmotic swelling, the levels of shear strain are on the order of 0.1 or less over the entire cell surface. With a radius of curvature scale on the order of 10^{-4} cm and a value of 6.6×10^{-3} dyn/cm for the shear modulus (Waugh and Evans, 1979), the ratio of bending to shear rigidity is calculated to be >0.3 for the osmotic swelling experiment but <0.01 for the pipet experiment. The difference in these values shows that the relative influence of bending and shear rigidities depends on the nature of the cell deformation. Not only is the buckling experiment useful for determination of the normal bending modulus, but it can also be used to discriminate between changes in bending and shear elasticities due to membrane alteration (e.g., diamide cross-linking treatment, Fischer et al., 1981).

It should be emphasized that in both the analysis and the micropipette experiment, isotropic tension was ignored because the pressure difference between the inside of the cell and external medium could be neglected. However, if the pressure inside the cell is significantly increased, then the cell surface will approach a spherical conformation and isotropic tension becomes important. Isotropic tension acts to stabilize the membrane against buckling (or folding), because it reduces the compressive membrane force resultant.

This work was supported in part by National Institutes of Health grant HL 26965.

Received for publication 22 June 1982 and in final form 17 January 1983.

REFERENCES

Chien, S., K.-L. P. Sung, R. Skalak, S. Usami, and A. Tozeren. 1978. Theoretical and experimental studies on viscoelastic properties of erythrocyte membrane. *Biophys. J.* 24:463–487.

Deuling, H. J., and W. Helfrich. 1976. Red blood cell shapes as explained on the basis of curvature elasticity. *Biophys. J.* 16:861–868.

Evans, E. A. 1973 *a*. A new material concept for the red cell membrane. *Biophys. J.* 13:926–940.

Evans, E. A.1973 *b*. New membrane concept applied to the analysis of fluid shear- and micropipette-deformed red blood cells. *Biophys. J.* 13:941–954.

Evans, E. A. 1980. Minimum energy analysis of membrane deformation applied to pipet aspiration and surface adhesion of red blood cells. *Biophys. J.* 30:265–284.

Evans, E. A., and R. Skalak. 1980. Mechanics and Thermodynamics of Biomembranes. C.R.C. Press, Inc., Boca Raton, FL.

Fischer, T. M., C. W. M. Haest, M. Stöhr-Liesen, H. Şchmid-Schönbein, and R. Skalak. 1981. The stress-free shape of the red blood cell membrane. *Biophys. J.* 34:409–422.

Hochmuth, R. M., N. Mohandas, and P. L. Blackshear, Jr. 1973. Measurement of the elastic modulus for red cell membrane using a fluid mechanical technique. *Biophys. J.* 13:747–762.

Jenkins, J. T. 1977. Static equilibrium configurations of a model red blood cell. *J. Math. Biol.* 4:149–169.

Schmid-Schönbein, H., and P. Gaehtgens. 1981. What is red cell deformability? *Scand. J. Clin. Lab. Invest. Suppl.* 156:13–26.

Waugh, R., and E. Evans. 1979. Thermoelasticity of red blood cell membrane. *Biophys. J.* 26:115–131.

Zarda, P. R., S. Chien, and R. Skalak. 1977. Elastic deformations of red blood cells. *J. Biomech.* 10:211–221.